1-1-2008

Elimination of gamma nonlinear luminance effects for digital video projection phase measuring profilometers

Matthew J. Baker
University of Wollongong, matthewb@uow.edu.au

Jiangtao Xi
University of Wollongong, jiangtao@uow.edu.au

Joe F. Chicharo
University of Wollongong, chicharo@uow.edu.au

Elimination of gamma nonlinear luminance effects for digital video projection phase measuring profilometers

Abstract

In this paper we are concerned with the elimination of gamma related errors by employing a simple and direct approach, specifically, for phase measuring profilometry (PMP) methods. The harmonic structure of a gamma distorted fringe is investigated and the implications of j for the PMP algorithm is studied. The minimum requirements in terms of number of Steps for appropriate elimination of j related phase residuals is identified and verified via both simulation and practical experimentation.

Keywords

Elimination, gamma, nonlinear, luminance, effects, for, digital, video, projection, phase, measuring, profilometers

Disciplines

Physical Sciences and Mathematics

Publication Details

Baker, M., Xi, J. & Chicharo, J. F. (2008). Elimination of gamma nonlinear luminance effects for digital video projection phase measuring profilometers. Fourth IEEE International Symposium on Electronic Design, Test and Applications (pp. 496-501). Los Alamitos, CA: IEEE Computer Society.

Elimination of γ Non-linear Luminance Effects for Digital Video Projection Phase Measuring Profilometers

M. J. Baker, J. Xi and J. F. Chicharo
School of Electrical, Computer and Telecommunications Engineering,
University of Wollongong, NSW 2522, Australia
Tel: +61 2 42 21 3244, Fax: +61 2 42 27 3277
E-mail: mjb06@uow.edu.au

***Abstract* – In this paper we are concerned with the elimination of γ related errors by employing a simple and direct approach, specifically, for Phase Measuring Profilometry (PMP) methods. The harmonic structure of a gamma distorted fringe is investigated and the implications of γ for the PMP algorithm is studied. The minimum requirements in terms of number of Steps for appropriate elimination of γ related phase residuals is identified and verified via both simulation and practical experimentation.**

***Keywords* – Gamma, Harmonics, Non-linear Luminance, Digital, Fringe, Focusing Profilometry, Defocus, PMP**

I. INTRODUCTION

Structured light techniques for non-contact, dynamic and accurate profile measurement of diffuse surfaces have been widely studied due to their potential industrial applications. The most exploited techniques often utilise a projected periodic sinusoidal fringe pattern composed of parallel lines. The phase of the observed sinusoid is modulated by the diffuse surface in such a way that the modulation contains information about the height of the object perpendicular to the plane of observation. The modulated structured light pattern is recorded, commonly by a CCD camera and then processed by a fringe processing algorithm to extract the spatial phase modulation. Figure (1) depicts the typical Crossed Optical Axes geometry utilised by many traditional structured light profilometers. Noting that triangle E_pE_cD and triangle ACD are similar and furthermore assuming system parameters d_0 and l_0 are known, the spatial phase modulation is thereby used to determine spatial distance AC and reconstruct the surface of interest in three-dimensional space.

$$\frac{AC}{-h(x,y)} = \frac{d_0}{l_0 - h(x,y)}$$

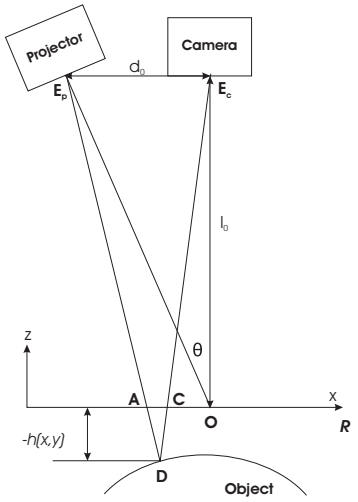

Fig. 1. TYPICAL CROSSED OPTICAL AXES PROFILOMETRY ARRANGEMENT

$$h(x,y) = \frac{l_0 AC}{AC - d_0}, \quad (1)$$

Traditionally, structured light fringe patterns are often generated using interferometric methods. An alternative to conventional interferometric techniques is Digital Video Projection (DVP). DVP is a technology which has been actively pursued in this particular field of research as it can provide a number of key advantages. For instance, typical digital video projectors are capable of projecting standard 24 bit bitmap computer generated images and hence, when interfaced to a personal computer make a very affordable, flexible and

0-7695-3110-5/08 $25.00 © 2008 IEEE
DOI 10.1109/DELTA.2008.90

robust projection source. However, for well exploited fringe processing algorithms such as Phase Measuring Profilometry (PMP) [1], nonlinear luminance effects commonplace with DVP significantly hinder the estimation of spatial displacement AC and hence system accuracy. Commonly, the nonlinear luminance associated with DVP is referred to as Gamma distortion. Gamma distortion is typical in visual display systems to enhance human perception of the sensation of *lightness*, which can be regarded as a power function of intensity [2].

Gamma correction for DVP based structured light profilometers was first identified by Guo *et al.* in [3] whereby the iterative statistical analysis of digital fringe patterns was undertaken to correct the Gamma distortion in digitally projected images. Through successful identification of the projector γ value, Guo *et al.* were able to considerably reduce reconstruction errors. More common solutions to counter γ non-linearities typically involve photometric fringe calibration, whereby multiple intensity distributions varying over the full range of luminance values are recorded and a camera / projector luminance curve is fitted [4], [5]. While alternate solutions have also been shown to calibrate projected fringes using signal processing concepts [6], [7] and other look-up table methods [8].

Although the γ of a projection source can be readily compensated by a range of methods, all proposed solutions have the requirement for additional data and / or further computation. In this paper we are concerned with the elimination of γ related errors, specifically, for PMP methods, otherwise referred to in literature as Phase Stepping, by employing a much simpler and direct approach. To the author's knowledge there has been some ambiguity in regard to the resulting implications γ nonlinear luminance poses for the PMP algorithm [9]. Hence, a further ambition in this work is to clearly identify the minimum requirements in terms of number phase steps, needed for appropriate elimination of higher order harmonic components commonplace with PMP applications coined on DVP. Rather than relying on additional processing or data acquisition the proposed approach is reliant only on the inherent nature of the PMP algorithm and a simple fringe optimisation by defocus. The validity of the proposed approach is demonstrated via both simulation and also empirically.

II. Principle Phase Measuring Profilometry

The principle Phase Measuring Profilometry approach is centered around the projection and acquisition of N fringe images with each fringe of the sequence offset by a known phase shift ζ_n. The phase offset ζ_n between each consecutive fringe image is equally spaced over the spatial period of the fringe with

$$\zeta_n = 2\pi n/N; \text{ for n=0,1,2,...,N-1,} \tag{2}$$

The nth fringe of a sequence of N fringes can therefore be ideally given as

$$g_n(x,y) = a(x,y) + b(x,y)\cos[2\pi f_0 x + \varphi(x,y) + \zeta_n] \quad \text{for n=0,1,2,...,N-1,} \tag{3}$$

where $\varphi(x,y)$ is the spatial phase modulation corresponding to the projection surface and where $a(x,y)$ and $b(x,y)$ are spatially varying functions representing the direct and contrast components of the recorded fringe. Each of the captured fringe images are appropriately weighted and summed to remove the unwanted direct components to give a pair of orthogonal vectors. The two vectors still contain the unwanted amplitude modulation component $b(x,y)$, and thus by calculating the arctangent of the division of the pair, the required phase information can be obtained as shown in Equation (4).

$$\varphi(x,y) = -\arctan\left[\frac{\sum_{n=0}^{N-1} g_n(x,y)\sin(2\pi n/N)}{\sum_{n=0}^{N-1} g_n(x,y)\cos(2\pi n/N)}\right] \tag{4}$$

Once the required spatial phase modulation can be obtain the final task is to convert the phase measurement to a height value. Given that PMP processes AC as a spatial phase displacement, Equation (1) becomes

$$h(x,y) \approx -\frac{l_0}{2\pi f_0 d_0}\Delta\phi(x,y), \tag{5}$$

where

$$\Delta\phi(x,y) = \phi(x,y) - \phi_0(x,y), \tag{6}$$

and where $\phi(x,y)$ and $\phi_0(x,y)$ are the phase modulations relating to the diffuse surface to be profiled and the reference plane R respectively, for the case where $l_0 \gg h(x)$.

Observing Equation (4) and (5), it is quite clear that the mathematics governing the evaluation of spatial displacement AC and hence $h(x,y)$, requires the adequate generation and capture of pure sinusoidal fringe images. In practice for DVP based approaches it quickly becomes apparent that the signals acquired at the respective CCD's of the capture device are clearly not pure sinusoid signals due to projector γ distortion and hence the accuracy of the PMP reconstruction is inadvertently compromised.

III. Modeling a γ Distorted Fringe

In general, the gamma distortion of a digital display can be modeled using the simple power function seen in Equation (7)

$$w(x,y) = u(x,y)^{\gamma}, \text{ for } u \in [0,1] \tag{7}$$

where $u(x,y)$ is the normalised image delivered to the display device, $w(x,y)$ is the actual normalised image output intensity distribution and γ is typically a fractional value $1 < \gamma < 3$ specific to the display device. Considering the PMP scenario where we typically have the projection of a sinusoidal intensity distribution, Equation (7) becomes,

$$w(x,y) = [a + b\cos(2\pi f_0 x)]^{\gamma}, \tag{8}$$

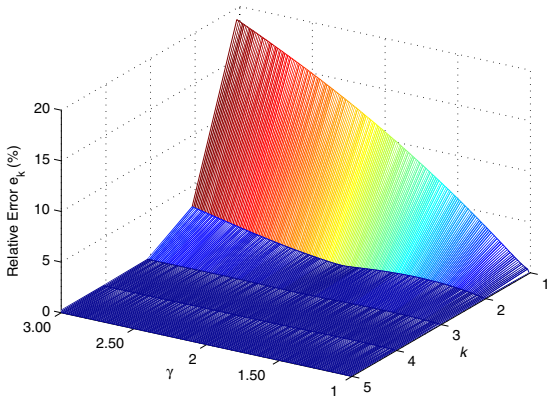

Fig. 2. e_k, $1 < \gamma < 3$, FOR NORMALISED FRINGE PARAMETERS $a = b$

where f_0 is the intended spatial carrier frequency of the projected fringe, and a and b are constants referring to the fringe offset and contrast respectively. Clearly, if γ is a fractional value and since $\cos(x)$ is an even function, we can represent Equation (8) as the following Fourier Series with infinite mth order harmonic components with corresponding amplitudes c_m.

$$w(x,y) = \left[c_0 + c_1 \cos(2\pi f_0 x) + \sum_{m=2}^{\infty} c_m \cos[m(2\pi f_0 x)] \right] \quad (9)$$

The obvious question on observation of Equations (8) and (9) is how to relate various c_m and γ to gain further understanding of the magnitude of harmonic distortion γ introduces. To demonstrate this we plot, e_k, the relative error of the kth order assumption of Equation (9) for the typical range of values for γ for a high contrast fringe with normalised fringe offset and contrast given by $a = b$. As indicated by Figure (2) the 3rd order assumption gives a good approximation for the gamma distorted fringe and hence all other higher order terms can be neglected and our approximation of the gamma distorted fringe becomes

$$\bar{w}(x,y) = \Big[a + b\cos(\theta) + c\cos(2\theta) + d\cos(3\theta) \Big] \quad (10)$$

where θ denotes the appropriate phase modulation term, $2\pi f_0 x + \varphi(x,y)$.

IV. INFLUENCE OF γ FOR PMP ALGORITHM

Now that we can appropriately model the gamma distorted fringe we can now gauge the influence the gamma distortion of a projector has on the PMP algorithm. Similar to much of the current research being undertaken in the 3D sensing area in this work we are ultimately concerned with dynamically profiling surfaces and, hence, we are primarily interested in reducing acquisition time and therefore PMP variations with low values of N. More specifically with $N = 3$ and $N = 4$.

Denoting $\hat{\varphi}(x,y)$ as the evaluation of the desired phase component, $\varphi(x,y)$, as calculated by substituting Equation (10) into (4) for a given value of N, we can obtain an expression for the residual phase measuring error introduced by the γ harmonics. We firstly consider the $N = 3$ case and it can be shown that the resulting estimation of $\varphi(x,y)$ can be given as

$$\hat{\varphi}(x,y) = \arctan\left[\frac{b\sin(\theta) - c\sin(2\theta)}{b\cos(\theta) + c\cos(2\theta)} \right] \quad (11)$$

and the resulting phase residual error can be given by

$$\delta(x,y) = -\arctan\left(\frac{\frac{c}{b}\sin(3\theta)}{1 + \frac{c}{b}\cos(3\theta)} \right) \quad (12)$$

Now repeating the process for $N = 4$,

$$\hat{\varphi}(x,y) = \arctan\left[\frac{b\sin(\theta) - d\sin(3\theta)}{b\cos(\theta) + d\cos(3\theta)} \right] \quad (13)$$

and the resulting phase residual error can be given by

$$\delta(x,y) = -\arctan\left(\frac{\frac{d}{b}\sin(4\theta)}{1 + \frac{d}{b}\cos(4\theta)} \right) \quad (14)$$

As shown in Equations (11) and (13) the PMP algorithm for the $N = 3$ case is insensitive to the 3rd order contribution, and sensitive to the 2nd order harmonic, while the $N = 4$ case is insensitive to the 2nd order, but sensitive to the 3rd order harmonic. Therefore, considering $c \gg d$ due to the nature of the γ term in Equation (8), the $N = 4$ PMP case is certainly less sensitive to gamma distortion for DVP based sensing.

Despite being insensitive to the 2nd order component the 4 Step PMP approach is still vulnerable to 3rd order harmonic distortions, furthermore, considering the overall γ of the projection system is typically not only a function inherent to the projector but also of the video card driving the projector, larger values of γ resulting in larger d are inevitable. Hence, a further attenuation of higher order terms is required to ensure the phase residual as specified by Equation (14) is eliminated.

V. ATTENUATING HIGHER ORDER HARMONICS

Generally, when a signal presents unwanted high frequency content, the desired low frequency components of the signal can be retrieved by employing some form of analytical low-pass filtering. In this particular scenario our filtering approach is centered on appropriately defousing the projection optics to attenuate the unwanted higher order terms. The application of defocusing projection optics to optimise projected fringe images is by no means a new concept, with Coggrave and Huntley [10] demonstrating a focused based optimisation of the

"Screen Door Effect" for a 3D sensor based on digital projection. Furthermore, Su *et al.* showed that a defocused Ronchi grating could be utilised as a formidable sinusoidal substitute in the PMP algorithm in [11]. The primary advantage of this very simple yet practical filtering approach is that it presents no further computational burden at the reconstruction stage. The derivation presented here follows that of Su *et al.* [11].

Assuming the typical digital video projector aperture is rectangular, the point spreading function otherwise referred to as the projection system impulse response can be given by

$$t(x) = rect\left(\frac{x}{a}\right) \tag{15}$$

where a is the width of the aperture. Therefore, the fringe image formed at the detector can be given by

$$\hat{w}(x,y) = \bar{w}(x,y) * rect\left(\frac{x}{a}\right) \tag{16}$$

To demonstrate the spatial frequency attenuation we derive the optical transfer function of the projection optics by taking the Fourier Transform of the point spread function seen as Equation (15)

$$T(f) = \frac{\sin(\pi a f)}{\pi a f} \tag{17}$$

If we now introduce a defocusing parameter, β,

$$\beta = a f_0 \tag{18}$$

and the frequency term $f = k f_0$, Equation (17) can be rewritten as

$$T(k f_0) = \frac{\sin(\pi \beta k)}{\pi \beta k} \tag{19}$$

As $\beta \rightarrow 1$ the integral of Equation (19) decreases and the first zero approaches the fundamental component i.e. $k = 1$ and the origin or dc component and therefore concentrates more energy in the central peak of the $sinc$ function. Hence, rewriting Equation (16) the defocused gamma distorted fringe can be given by

$$\begin{aligned} \hat{w}(x,y) \quad = \quad & \Big[a + T(f_0).b\cos(\theta) + T(2f_0).c\cos(2\theta) + \\ & T(3f_0).d\cos(3\theta)\Big] \end{aligned} \tag{20}$$

where the coefficients $T(k f_0)$ decay according to Equation (19) providing the desired low-pass filtering effect.

VI. Simulation

In order to verify the validity of the analytical findings including the proposed fringe optimisation by defocus, we simulated a series of defocused γ distorted fringes projected onto a test surface and measure the surface using the 3 Step and 4 Step variations of the PMP algorithm. To demonstrate the effectiveness of the approach and emulate the maximum harmonic distortion conditions of a typical DVP system, the values of γ and fringe offset and contrast parameters were selected to be 3 and $a = b$, respectively. According to Equation (19) we calculated the $T(k f_0)$ coefficients, some of which are shown in Table (I). To ensure the simulation provided as much insight in the practical application of defocusing, β was selected to be 0.3, since the attenuation in the fundamental component is minimal relative to the 2nd and 3rd order components given that SNR is an important consideration for practical situations.

β	$T(f_0)$	$T(2f_0)$	$T(3f_0)$
0.1	0.9836	0.9355	0.8584
0.2	0.9355	0.7568	0.5046
0.3	0.8584	0.5046	0.1093
0.4	0.7568	0.2339	0.1559

TABLE I.
VARIOUS β AND THE CORRESPONDING GAIN COEFFICIENTS $T(k f_0)$ FOR $k = 1, 2, 3$.

PMP ($N = 3$)	$\gamma = 3$		
	$\epsilon\ (mm)$	$\delta\ (mm)$	$\epsilon_{MAX}\ (mm)$
Focused	6.6212	7.0163	32.4318
Defocused	3.8419	4.0781	18.7615
PMP ($N = 4$)	$\gamma = 3$		
	$\epsilon\ (mm)$	$\delta\ (mm)$	$\epsilon_{MAX}\ (mm)$
Focused	1.0901	1.1572	5.1995
Defocused	0.1388	0.1474	0.6638

TABLE II.
MEAN ERROR (ϵ), STANDARD DEVIATION (δ) AND MAXIMUM ABSOLUTE ERROR (ϵ_{MAX}) IN MM FOR THE PMP 3 AND 4 STEP ALGORITHMS FOR BOTH THE FOCUSED AND DEFOCUSED CASES WITH $\gamma = 3$

System parameters l_0, d_0 and f_0 were chosen to be 5m and 2m and 10/m respectively, corresponding to a spatial period of 100mm if we assume an image spatial resolution of 1pixel/mm. The test surface is a hemispherical convex shape with a diameter of 800mm and maximum height of 160mm corresponding to a maximum phase displacement 4.154 rads. The reconstructed surfaces for the 3 and 4 Step PMP algorithms for both the focused and defocused cases are displayed in Figures (3) (a), (b), (c) and (d) respectively. Table (II) displays the Mean Error (ϵ), Standard Deviation (δ) and Maximum Absolute Error (ϵ_{MAX}) in mm for both the PMP 3 and 4 Step algorithms for both the Focused and Defocused cases. Clearly, as anticipated the 4 Step defocused case almost completely eliminates the systematic reconstruction errors associated with the γ term.

VII. Empirical Verification

To verify the physical application of the PMP fringe optimisation approach, practical experimental results were established via the profiling of a convex dome shape mounted on a flat board. The maximum height of the hemispherical

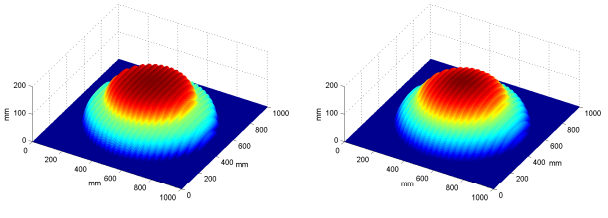

(a) 3 Step Focused (b) 3 Step Defocused

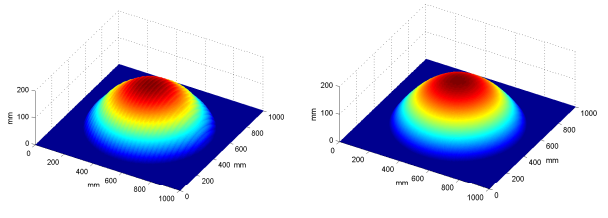

(c) 4 Step Focused (d) 4 Step Defocused

Fig. 3. SIMULATED RECONSTRUCTIONS

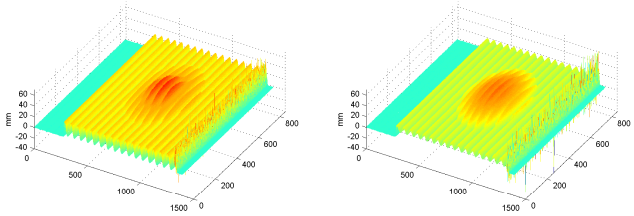

(a) 3 Step Focused (b) 3 Step Defocused

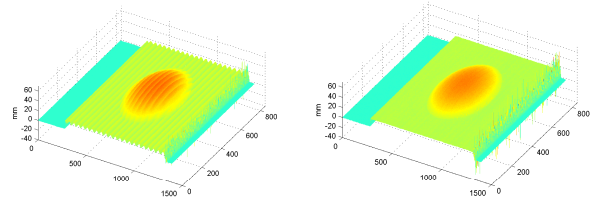

(c) 4 Step Focused (d) 4 Step Defocused

Fig. 4. EMPIRICAL RECONSTRUCTIONS

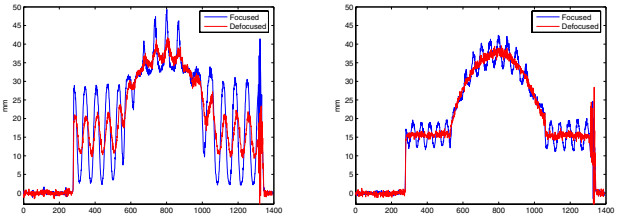

(a) 3 Step Focused (b) 3 Step Defocused

Fig. 5. CROSS-SECTIONS OF EMPIRICAL RECONSTRUCTIONS

shape was known to be approximately 22.8mm with a diameter of 99mm, with the thickness of the base material being 16mm. Our projection system is composed of a Hitachi CP-X260 LCD digital video projector interfaced to a dual head matrox video card. Similar to the simulation we emulated maximum harmonic distortion conditions by projecting a high contrast fringe with the γ value on the video card set to 3 in software. The fringes were recorded using a MS3100 3-CCD camera with an effective resolution of 1039x1392. The surface was reconstructed using both the 3 and 4 Step variations of the PMP algorithm for both the focused and defocused scenarios. The 3D reconstructions are shown in Figures (4) (a)-(d) while Figures (5) (a) and (b) display an arbitrary cross-section of the 3 and 4 Step reconstructions for both the focused and defocused cases, respectively.

An important aspect to note in each of the defocused cases is the reduced SNR. Given our experiment was adjusted to produce a large harmonic distortion, the amount of required attenuation by defocusing was also increased accordingly. Considering the typical practical situation where the harmonic distortion is likely to be less significant, the diminishing SNR due to significant defocusing is likely to be much less influential. Nevertheless, the practical low-pass effectiveness of defocusing the projection optical system to attenuate fringe γ distortion is clearly demonstrated.

VIII. CONCLUSION

In this paper we have investigated the operation of the PMP algorithm in the presence of gamma distortion commonplace with DVP implementations. The harmonic structure of a γ distorted fringe was investigated and an appropriate model for a γ distorted fringe was discussed. Analytical investigation into the implications γ has on the PMP algorithm were demonstrated and contrary to previously published works it was concluded via simulation and empirically that the minimum requirement to adequately eliminate γ related phase residuals is the 4 Step PMP variation combined with a simple defocusing fringe optimisation approach.

REFERENCES

[1] V. Srinivasan, H. C. Lui, M. Halioua, "Automated phase-measuring profilometry of 3-d diffuse objects," *Applied Optics*, vol. 23, pp. 3105–3108, 1984.

[2] C. A. Poynton, "Gamma and it disguises: The nonlinear mappings of intensity in perception, crts, film and video," *SMPTE Journal*, pp. 1099–1108, 1993.

[3] H. Guo, H. He, M. Chen, "Gamma correction for digital fringe projection profilometry," *Applied Optics*, vol. 43, no. 14, pp. 2906 – 2914, May 2004.

[4] L. Kinell, "Multichannel method for absolute shape measurement using projected fringes," *Optics and Lasers in Engineering*, vol. 41, pp. 57–71, 2004.

[5] P. S. Huang, Q. Hu, F. Jin, F. Chiang, "Color-encoded digital fringe projection technique for high speed three-dimensional surface contouring," *Optical Engineering*, vol. 38, pp. 1065–1071, 1999.

[6] M. J. Baker, J. Xi, J. F. Chicharo, "Neural network digital fringe

calibration technique for structure light profilometers," *Applied Optics*, vol. 46, no. 8, pp. 1233–1243, March 2007.

[7] H. Zhi, R. B. Johansson, "Adaptive filter for enhancement of fringe patterns," *Optics and Lasers in Engineering*, vol. 15, pp. 241–251, 1991.

[8] S. Zhang and S. Yau, "Generic nonsinusoidal phase error correction for three-dimensional shape measurement using a digital video projector," *Applied Optics*, vol. 46, no. 1, pp. 36–43, January 2007.

[9] P. S. Huang, Q. J. Hu and F. Chiang, "Double three-step phase-shifting algorithm," *Applied Optics*, vol. 41, no. 22, pp. 4503–4509, August 2002.

[10] C. R Coggrave and J. M. Huntley, "Optimization of a shape measurement system based on spatial light modulators," *Optical Engineering*, vol. 39, no. 1, pp. 91–98, January 2000.

[11] X. Su, W. Zhou, G. Bally and D. Vukicevic, "Automated phase-measuring profilometry using defocused projection of a ronchi grating," *Optics Communications*, vol. 94, pp. 561–573, 1992.